

Article

Preparation of Side-By-Side Bicomponent Fibers Using Bio Polyol Based Thermoplastic Polyurethane (TPU) and TPU/Polylactic Acid Blends

Jiyeon Oh ¹, Young Kwang Kim ¹, Sung-Ho Hwang ¹, Hyun-Chul Kim ², Jae-Hun Jung ³, Cho-Hyun Jeon ⁴, Jongwon Kim ⁵ and Sang Kyoo Lim ^{1,6,*}

¹ Division of Energy Technology, Daegu Gyeongbuk Institute of Science and Technology (DGIST), Daegu 42988, Korea

² Division of Biotechnology, Daegu Gyeongbuk Institute of Science and Technology (DGIST), Daegu 42988, Korea

³ Living Materials Research Lab, Korea Textile Development Institute (KTDI), Daegu 41842, Korea

⁴ Eco-Friendly Materials Team, Korea Textile Development Institute (KTDI), Daegu 41842, Korea

⁵ Department of Fiber System Engineering, Yeungnam University, Gyeongsan 38541, Korea

⁶ Department of Interdisciplinary Engineering, Daegu Gyeongbuk Institute of Science and Technology (DGIST), Daegu 42988, Korea

* Correspondence: limsk@dgist.ac.kr

Abstract: In this study, side-by-side bicomponent fibers were prepared by melt spinning using bio-based thermoplastic polyurethane (TPU) and TPU/polylactic acid (PLA) blends. The morphology, thermal and mechanical properties of the fibers were investigated. To this end, the synthesis of TPU using biomass-based polyols and the preparation of TPU/PLA blends were preceded. Their morphological and structural characteristics were investigated. The synthesis of TPU was confirmed through Fourier transform infrared analysis, and as a result of gel permeation chromatograph analysis, a compound having a weight average molecular weight of 196,107 was synthesized. The TPU/PLA blends were blended in the ratio of 80/20, 60/40, 40/60, and 20/80 through a melt extruder. They formed a sea-island structure as a result of scanning electron microscope analysis, and an increase in the PLA content in the TPU matrix caused a decrease in the melt flow index. Finally, TPU/(TPU/PLA) side-by-side bicomponent fibers were prepared by utilizing the above two materials. These fibers exhibited tensile strengths of up to 3624 MPa, with improved biocarbon content of up to 71.5%. These results demonstrate the potential of TPU/(TPU/PLA) side-by-side bicomponent fibers for various applications.

Keywords: bio-based polyester polyols; thermoplastic polyurethane; polylactic acid; side-by-side bicomponent fiber; melt spinning



Citation: Oh, J.; Kim, Y.K.; Hwang, S.-H.; Kim, H.-C.; Jung, J.-H.; Jeon, C.-H.; Kim, J.; Lim, S.K. Preparation of Side-By-Side Bicomponent Fibers Using Bio Polyol Based Thermoplastic Polyurethane (TPU) and TPU/Polylactic Acid Blends. *Fibers* **2022**, *10*, 95. <https://doi.org/10.3390/fib10110095>

Academic Editor: Andou Yoshito

Received: 6 October 2022

Accepted: 3 November 2022

Published: 9 November 2022

Publisher's Note: MDPI stays neutral with regard to jurisdictional claims in published maps and institutional affiliations.



Copyright: © 2022 by the authors. Licensee MDPI, Basel, Switzerland. This article is an open access article distributed under the terms and conditions of the Creative Commons Attribution (CC BY) license (<https://creativecommons.org/licenses/by/4.0/>).

1. Introduction

Petroleum-based polymers have been utilized as significant materials in many applications due to their excellent properties and ease of processing, both thermosetting and thermoplastic polymers [1]. However, with the expected depletion of fossil energy and environmental problems due to increasing carbon and greenhouse gas emissions, the need for the development of eco-friendly biomass-based polymers is required [2]. Therefore, bio-based thermoplastic polymers can be one of the potential alternatives to conventional petroleum-based polymers and composites as they have a very low environmental impact [3–5].

Thermoplastic polyurethane (TPU) is an important polymer that combines the soft and elastic properties of rubber with the easy processing performance of thermoplastics [6]. The TPU chain is usually composed of soft segments (SS) and hard segments (HS), and the SS providing elasticity and HS providing mechanical stability give the TPU material

its unique properties [7]. In general, HS is made of a rigid diisocyanate and a chain extender such as diols, whereas SS is mainly composed of a soft long polyol [8]. Because TPU has many advantages such as simple processing technology, recyclability, excellent thermal properties [9,10], and biocompatibility [11,12], it is used in various fields [13–15]. However, so far, the main starting material for TPU is still derived from non-renewable fossil fuels [16,17]. Therefore, bio polyol derived from vegetable oil, not from petroleum, can be to TPU with improved bio-contents [18–20].

Thermoplastic polymers can further improve their bio-content through blending with fully renewable biopolymers. Among them, polylactic acid (PLA) is one of the most important thermoplastic biopolymers having an aliphatic polyester structure. It is a material with superior biodegradability and high mechanical properties compared to other biopolymers [1]. Polyester polyol-based TPU and PLA have partial compatibility due to intermolecular hydrogen bonding [21,22]. For this reason, research on improving the physical properties of the composite through the general TPU/PLA blends has been steadily progressing. Jašo et al. [23] prepared reinforced TPU/PLA blends with 200–800 nm fibrils by blending 10–40 wt% PLA microfibers in a TPU matrix. Hong et al. [24] showed that the addition of TPU elastomer to PLA can progressively transform brittle fractures into ductile fractures. Feng et al. [14] blended PLA with 20 wt% TPU to improve elongation at break and notch impact strength by 350% and 25 kJ/m, respectively.

According to the literature review, studies so far have focused on the blending of TPU and PLA and mainly analyzed the effects. The field of application must also be considered for the wide use of TPU/PLA blends that can replace the existing petroleum-based plastic polymers. However, according to our investigation, there are no studies on the preparation and properties of side-by-side bicomponent fibers that can be used in various industries by applying bio-based TPU/PLA blends. Bicomponent fibers are a type of composite fiber and are also commonly known as “conjugated fibers”. A fiber is formed by two different polymers, each molten and fed to a different spinning channel and finally extruded from the same nozzle hole [25–27]. This method makes it possible to prepare fibers with various properties in which the advantages of the two raw materials are combined [28]. Among them, side-by-side bicomponent fibers are fibers in which two types of polymers having different shrinkage rates or melt viscosities are distributed adjacently along the fiber axis [29–31].

However, the difference between the two components constituting side-by-side should not be too large, and compatibility should be somewhat satisfied. Otherwise, the two parts will not be able to withstand excessive mechanical forces during processing, as the adhesion between the two parts may not be sufficient and may cause separation [32]. Therefore, in this study, a TPU/(TPU/PLA) side-by-side bicomponent fiber with improved physical properties was prepared using a TPU and TPU/PLA blend to ensure compatibility between the two components. The TPU/(TPU/PLA) side-by-side bicomponent fiber consists of TPU and TPU/PLA blends. The presence of the same component, TPU, in the bicomponent fiber may impart miscibility between the interfaces. In the case of fibers in which the TPU and TPU/PLA blend form a continuous phase at the interface of two components, an increase in the PLA content of the TPU/PLA blend is expected to bring about an improvement in tensile strength.

For the production of these side-by-side bicomponent fibers, the preparation and characterization of the constituent components were preceded step by step. First, the synthesis and structural characterization of TPU based on bio-polyester polyol was performed, and then, by blending with PLA of specific contents, TPU/PLA blends were prepared. The contents of the TPU/PLA blends were 80/20, 60/40, 40/60, and 20/80, and the morphological characteristics of the blends were observed. Various properties of TPU/(TPU/PLA) side-by-side bicomponent fibers finally prepared using them were analyzed. Fourier transform infrared (FT-IR), scanning electron microscope (SEM), differential scanning calorimeter (DSC), and tensile properties were studied.

2. Materials and Methods

2.1. Materials

Bio-based polyester polyols with number average molecular weights (M_n) of 1000 and 2000 g/mol, respectively, and 4,4'-methylene diphenyl diisocyanate (MDI, CAS No. 101-68-8) were provided by Union chemicals (Bucheon, Korea). The provided polyester polyols were synthesized from 1,3-propanediol (CAS No. 504-63-2) and sebacic acid raw material (CAS No. 110-20-6). When synthesizing TPU, 1,4 butanediol (BDO, Daejung, Siheung, Korea, CAS No. 110-63-4) was used as a chain extender. Other auxiliaries such as catalyst (stannous octoate, CAS No. 301-10-0) and heat stabilizer (triphenyl phosphite, CAS No. 3076-63-9) were provided by Sambu Fine Chemicals (Gimhae, Korea). TPU Bio-60D 220719E (Sambu Fine Chemical, Gimhae, Korea) and PLA LX 175 (TotalEnergies Corbion, Gorinchem, The Netherlands) containing 96% L-isomer were used as spinning resins.

2.2. Methods

For the production of TPU/(TPU/PLA) side-by-side bicomponent fibers through melt spinning, the fabricating process of TPUs and TPU/PLA blends, which are the main raw materials, was preceded. First, bio-polyester polyol-based TPU was synthesized, and then TPU/PLA blends were prepared for each PLA content. Detailed procedures for each step are presented below.

2.2.1. Synthesis of Biomass-Based TPU

TPUs were synthesized based on bio-polyester polyols through a one-shot polymerization process, which does not use solvents and has environmental advantages [33]. The bio-polyester polyol was heated in a vacuum oven at 80 °C for 2 h, and MDI was melted in an oven at 70 °C for 2 h. A completely molten polyester polyol, BDO, was placed in a polytetrafluoroethylene (PTFE) reaction vessel and mechanically stirred at 80 °C. To this was added about 0.2 wt% of thermal stabilizer and catalyst. Then, an appropriate amount of MDI was slowly added by adjusting the molar ratio of polyol/BDO/MDI to 1/1/2. It was carried out under nitrogen purge conditions to prevent a reaction between moisture in the air and isocyanate. After the temperature was stabilized by the reaction of the polyester polyol with isocyanate, stirring was continued at 80 °C and 400 rpm for 1 h resulting in a large increase in viscosity of the TPU. Then, the polymer after polymerization in the vessel was poured onto a thin layer of PTFE film and heated in an oven at 80 °C for one day. This was to ensure the complete reaction of the isocyanate groups and the results were further monitored by FT-IR [34]. The polymerization process is detailed in Figure 1.

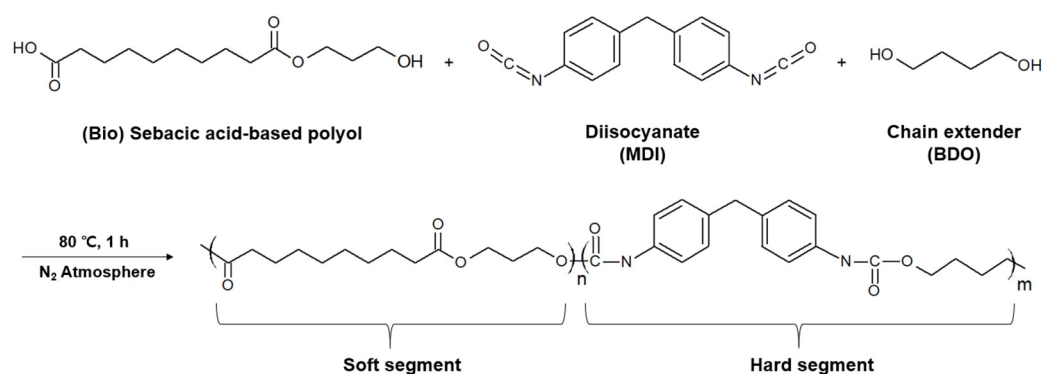


Figure 1. Schematic diagram of TPU synthesis mechanism.

2.2.2. Preparation of TPU/PLA Melt Blends

TPU and PLA resins were dried in a vacuum oven at 100 °C and 85 °C, respectively, for 4 h. The dried TPU and PLA were quantified and mixed in a quantitative ratio of 80/20, 60/40, 40/60, and 20/80, and then supplied to a Rhomex CTW 100 OS Twin-Screw Extruder (HAAKE, Paramus, NJ, USA). The inner extruder barrel and die temperatures were set at 210,

220, 225, 230, 230, 230, and 225 °C, and the twin-screw speed was set at 80 rpm. The blend strands extruded through a 6 mm die were passed directly through a coagulation bath filled with water and pelletized using a Pelletizer 557-2684 (STONE, Stafford-shire, UK).

2.2.3. Melt Spinning of TPU/(TPU/PLA) Side-By-side Bicomponent Fibers

The TPU resin and the TPU/PLA blend for each ratio were dried in a vacuum oven at 85 °C for 3 h for the fiber spinning process (Figure 2) and then put into KSP SDY (Tmt Machinery, Osaka, Japan), respectively. The extruder's internal temperature was set to 210, 220, 220, 220, 230, 230, and 230 °C. TPU resin was fed to one hopper, and TPU/PLA blends in 80/20, 60/40, 40/60, and 20/80 ratios were provided to the other hopper. Then, the fiber strands spun along the side-by-side spinneret were directly drawn by godet rollers at 60 and 80 °C at 800 and 1400 mpm and then wound. Then, TPU/(TPU/PLA) side-by-side bicomponent fibers of 150 denier/12 filament specifications were prepared.

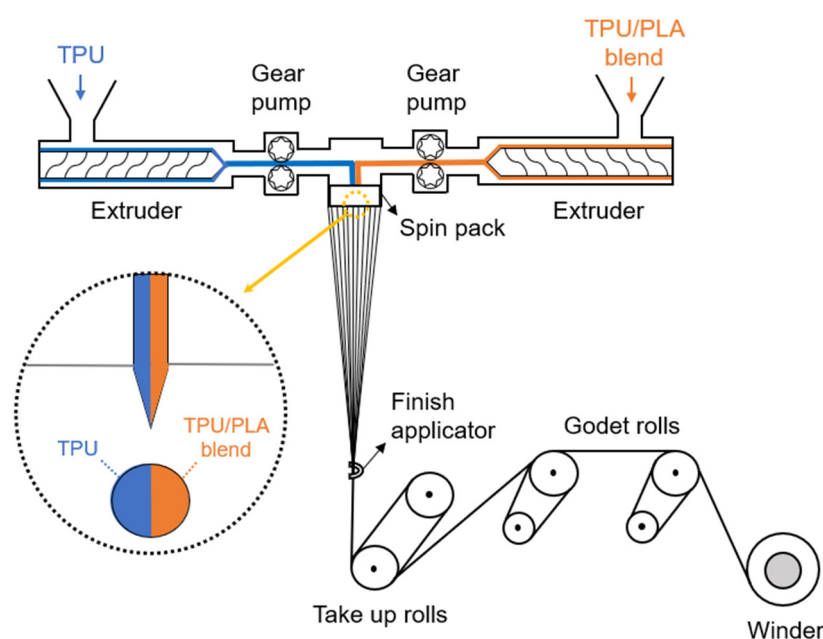


Figure 2. Schematic diagram of the preparation of TPU/(TPU/PLA) side-by-side bicomponent fibers.

2.2.4. Characterization

Gel permeation chromatography (GPC) analysis was performed through Ecosec GPC (Tosoh Company, Tokyo, Japan) to measure the number average molecular weight (M_n), weight average molecular weight (M_w), and polydispersity index (PDI) of the TPU samples. The sample solution for analysis was prepared by adding 50 mg of dried polymer to 5 mL of inhibitor-free tetrahydrofuran solution, completely dissolving it at room temperature for one day, and then filtering it with a 0.45 μm PTFE filter [35]. The HS content of the TPU samples was calculated as a percentage of the mass of the chain extender and isocyanate making up the HS out of the total mass of all starting materials [36]. Biomass content was measured according to standard ASTM D6866-20. All samples were used for measurement graphitization. The instrument reported raw percent Modern Carbon (pMC) results for each test sample on the isotopic ratio of ^{14}C to ^{12}C . These test results were then adjusted for the ^{13}C to ^{12}C isotopic ratio reported by the instrument at the time of measurement. The adjusted pMC values were assigned a carbon year and adjusted further using Equation (1) to obtain an uncorrected biobased carbon content:

$$\% \text{Biobased C} = \frac{\text{pMC}}{\text{Ref}} \times 100 \quad (1)$$

where %Biobased C stands for uncalibrated bio-based carbon from the test sample and pMC is the instrument's adjusted percent Modern Carbon result. Ref is the reference percent of Modern Carbon for the year atmospheric carbon was incorporated into biomass via photosynthesis. The reference value used for the carbon year adjustment was 100 pMC per ASTM D6866-20 [37].

FT-IR of all samples was performed through a Nicolet Continuum (Thermo Scientific Inc., Middlesex, MA, USA) with attenuated total reflection (ATR) mode. The spectra were collected in the range of 4000–500 cm^{-1} at a resolution of 4 cm^{-1} . SEM analysis was performed using an FE-SEM SU 8230 (Hitachi, Tokyo, Japan). Each sample was sputtered with gold prior to measurement. TPU/PLA blend samples were immersed in ethyl acetate (Samchun, Seoul, Korea, 99%) to dissolve PLA partially, and cross-sections were observed. Melt flow index (MFI) testing of this blend sample was also performed using an MFI QM280A (QMESYS Corp., Uiwang, Korea) at 210 °C under a 2.16 kg load, according to ASTM D1238.

Thermal characterization of the fiber samples was performed using a DSC model Q 2000 (TA Instruments, New Castle, DE, USA). Approximately 6 mg of samples were placed in an aluminum pan for measurement. It was carried out for one cycle at a heating/cooling rate of 10 °C/min at –80 to 230 °C in a nitrogen atmosphere. The crystallinity (X_c) was estimated using Equation (2). ΔH_m is the enthalpy of crystallization per gram of the sample, and $\Delta H_{m,0}$ is the enthalpy of crystallization per gram of 100% crystalline TPU. The latter was taken as 196.8 J/g [38,39].

$$X_c = \frac{\Delta H_m}{\Delta H_{m,0}} \times 100 \quad (2)$$

Mechanical property analysis was performed using a Universal Testing Machine model 5565 (Instron, Norwood, MA, USA) at a 50 mm gauge length and an extension speed of 100 mm/min. At least five specimens were tested for each sample material to obtain an average value.

3. Results and Discussion

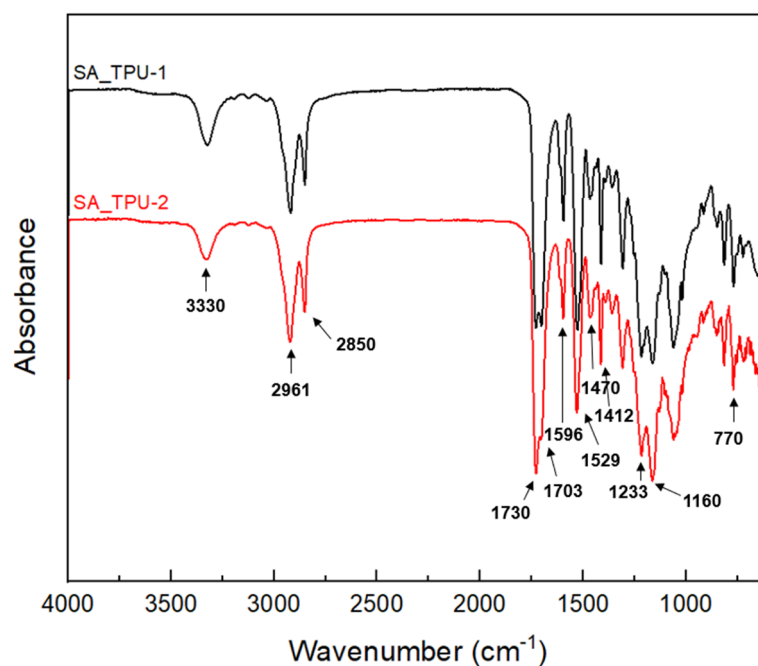
3.1. Characterization of TPU

Table 1 shows the M_w , M_n , and PDI of TPU samples based on bio-sebacic acid (SA) polyester polyol. SA_TPU-1 with an M_n of 1000 g/mol of the polyol used for TPU synthesis exhibited a higher average molecular weight than SA_TPU-2 with 2000 g/mol, and all PDI values satisfied two or less. In addition, the HS content of SA_TPU-1 synthesized with a low molecular weight polyol was 35.9%, which was higher than that of SA_TPU-2 at 22.1%. According to previous studies [40–42], the lower the molecular weight of the polyol used for TPU synthesis, the higher the HS fraction, which is consistent with our results in Table 1. In addition, when the HS content in TPU is about 25% or more, it shows a physical crosslinking effect through crystallization, thereby exhibiting desirable thermoplastic elastomer properties [43,44]. Through this, we could expect that SA_TPU-1 would have sufficient properties of a thermoplastic elastomer since it had an HS content of 25% or more. M_w of about 190,000 is also enough for use in polymer processing (e.g., extrusion, spinning) and commercial applications to make blends. Through this study, we successfully synthesized bio-polyol-based TPUs with higher M_w and M_n than in our previous study [35]. In an earlier work, CA_TPU-1 and CA_TPU-2 were synthesized using bio succinic acid (CA)-based polyester polyols with M_n of 1000 and 2000 g/mol. Compared with these samples, SA_TPU-1 and SA_TPU-2 have higher bio content as well as average molecular weight. According to another document [45], it was determined that the SA-based TPUs having more methylene groups had a higher bio content due to the difference in the number of methylene groups in the bio polyol.

Table 1. Molecular weight, polydispersity, HS content, and bio-content of TPU samples.

Samples	M _w (g/mol)	M _n (g/mol)	PDI (M _w /M _n)	HS Content (wt%)	Bio-Based C (%)	Reference
SA_TPU-1	196,107	94,030	2.0	35.9	54.8	This work
SA_TPU-2	136,489	89,659	1.5	22.1	56.1	This work
CA_TPU-1	120,158	88,125	1.3	38.8	54.1	[35]
CA_TPU-2	113,738	84,906	1.3	22.3	53.0	[35]

FT-IR analysis was used to confirm the termination of the reaction and the change in the functional groups during polymerization, and their spectra are shown in Figure 3. The complete reaction of the $-OH$ group and the $N=C=O$ group was confirmed by the disappearance of the 2270 cm^{-1} vibration table and the vibration of the urethane group [46]. The completion of TPU synthesis was confirmed by the presence of vibrations of 3330 cm^{-1} and 1529 cm^{-1} appearing due to the stretching and bending of $-NH$ bonds in urethane bonds. At about 1730 and 1703 cm^{-1} , peaks corresponding to the $C=O$ stretching of the urethane group were observed [34]. The 1596 and 1470 cm^{-1} peaks appeared due to the presence of a benzene group. The spectrum also contains a 1412 cm^{-1} absorption band that appears due to stretching vibrations of the $C-C$ aromatic benzene ring group [47]. The peak at 1233 cm^{-1} is due to the $C-O-C$ vibration of urethane, while the peak at 1160 cm^{-1} is assigned to the $C-O-C$ vibration of the ester group. The peak at 770 cm^{-1} comes from $C-O-O$ urethane vibrations [48,49]. Depending on the presence or absence of hydrogen bonding, the $C=O$ stretching vibration peaks of the urethane group show absorption bands at different positions at 1730 cm^{-1} (Free $C=O$ peak) and 1703 cm^{-1} (H-bonded $C=O$ peak), respectively [35]. As the HS content increases, the phase-separated structure becomes from isolated domains to interconnected domains. Therefore, the interfacial area between the two-phase is reduced, making it the HS domain easier to form hydrogen bonds [43,50]. Therefore, SA_TPU-1 with a high HS content showed a higher fraction of hydrogen-bonded $C=O$ peaks, which is consistent with the results of the GPC analysis.

**Figure 3.** FT-IR spectra of synthesized TPU samples.

3.2. Characterization of TPU/PLA Blends

Figure 4 shows the SEM cross-sectional shapes of TPU/PLA blends prepared with TPU and PLA at 80/20, 60/40, 40/60, and 20/80 ratios, respectively. At this time, the TPU was based on SA_TPU-1, which was selected based on the results of the previous section. Images of pure TPU and PLA were also included in Figure 4a and f, respectively. Both TPU and PLA showed no or little surface texture. Some PLA and TPU particles were lost during sample preparation for SEM observation at the fracture surface of the TPU/PLA blends, which left some shallow pores in the TPU and PLA matrix, respectively [51]. In the blends of (b) 80/20 and (e) 20/80 ratios of TPU/PLA, spherical PLA particles distributed throughout the TPU matrix showed a clear dual-phase sea-island structure. At this time, the higher the PLA content, the more spheres could be seen. TPU/PLA (c) 60/40 and (d) 40/60 blends showed co-continuous morphology of TPU and PLA. It was found that the phases of TPU and PLA were mixed, the spherical shape merged, and the size increased. This phenomenon is also in good agreement with previous studies [52,53].

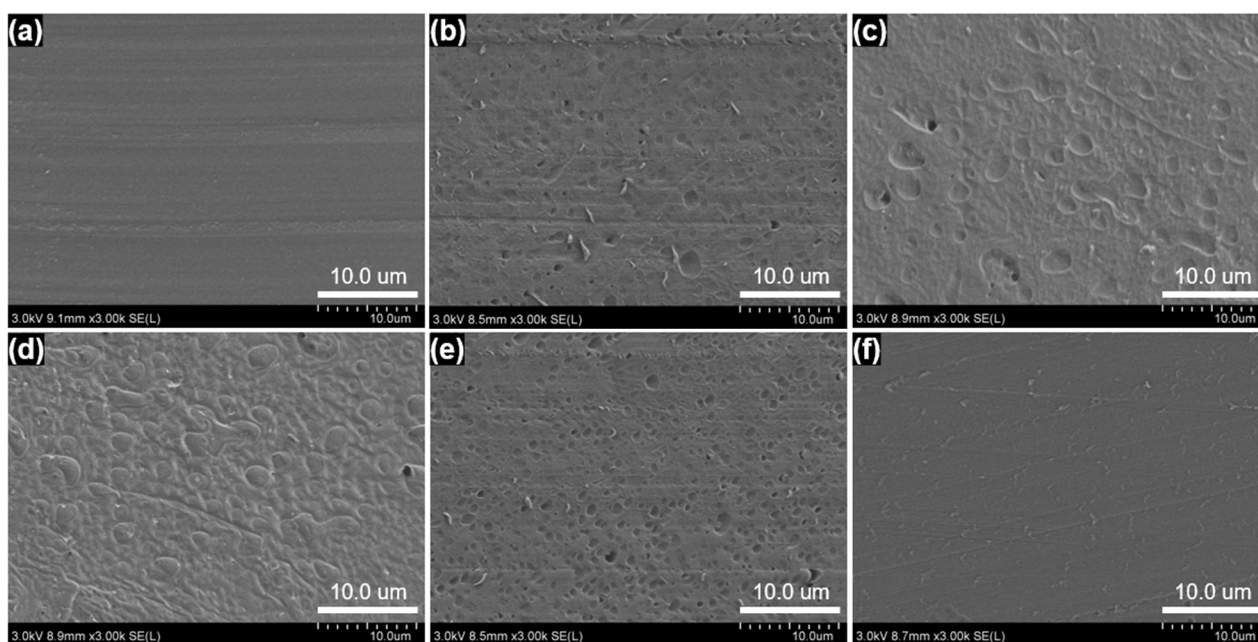


Figure 4. SEM images of TPU, TPU/PLA blends, and PLA: (a) TPU, (b) 80/20, (c) 60/40, (d) 40/60, (e) 20/80, and (f) PLA.

Figure 5 shows the cross-sectional shape with PLA removed to observe the co-continuous morphology of the blend better. In fact, after PLA removal, the TPU/PLA (a) 80/20 and (d) 20/80 blends showed a relatively regular spherical shape. On the other hand, the (b) 60/40 and (c) 40/60 blends had a spongy-like structure, suggesting a co-continuous conformation [14,22]. Through these results, it was confirmed that TPU and PLA can have some miscibility.

Figure 6 shows the MFI values for each ratio of TPU/PLA blends, including TPU and PLA. The MFI value of the blends is an important parameter for melt processability during the fiber spinning process [54]. The MFI value of the TPU/PLA blend steadily decreased with increasing PLA ratio compared to pure TPU, and it was found that the 20/80 ratio almost reached the MFI value of pure PLA. That is, it can be seen that the incorporation of PLA into TPU causes a decrease in MFI and an increase in melt viscosity. This difference in viscosity also affected the cross-sectional shape of the bicomponent fiber produced through melt spinning in the following process, which will be analyzed in detail in the next section.

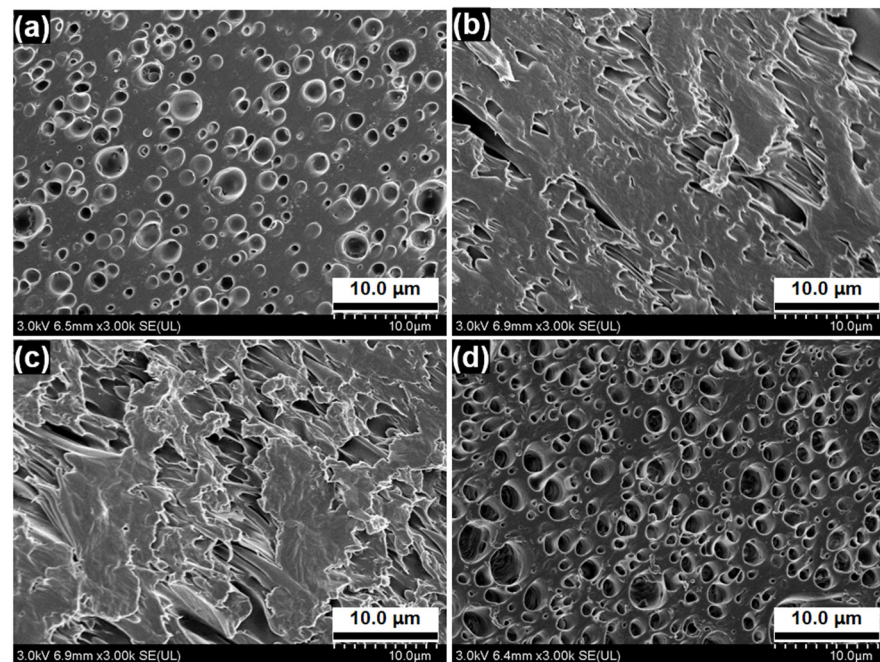


Figure 5. SEM image of TPU/PLA blends with PLA removed: (a) 80/20, (b) 60/40, (c) 40/60, and (d) 20/80.

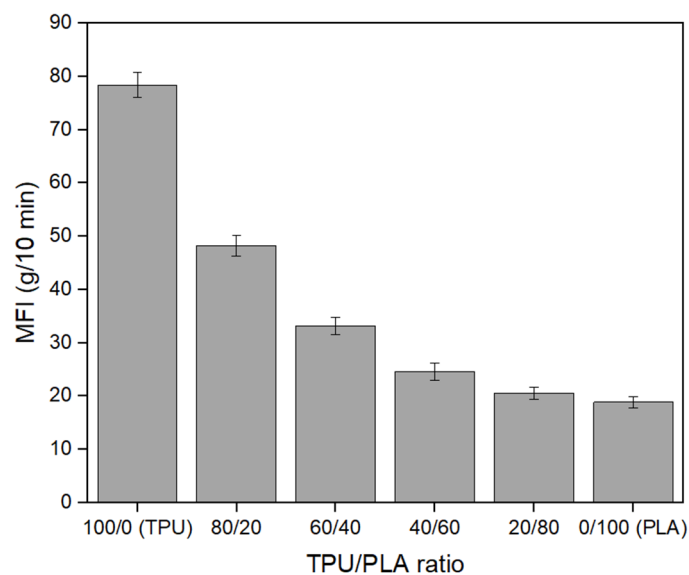


Figure 6. MFI test results of TPU, TPU/PLA blends, and PLA.

3.3. Characterization of TPU/(TPU/PLA) Side-By-Side Bicomponent Fibers

Side-by-side bicomponent fibers were prepared by melt spinning using TPU and a TPU/PLA blend as base materials. Moreover, also included were (e) TPU/PLA 50/50 side-by-side bicomponent fibers composed of pure TPU and PLA, respectively. The side-by-side cross-sectional shape of the actual samples was observed through SEM analysis and is shown in Figure 7. The interface between TPU and TPU/PLA showed a concave shape at the periphery of the TPU and a convex shape at the center of the TPU/PLA. This deformation is due to the viscous dissipation phenomenon [55]. Since TPU and TPU/PLA blends flow at different rates due to differences in viscosity, the low-viscosity component tends to encapsulate the high-viscosity component [32,56]. Based on the MFI results in the previous section, it can be seen that the high-viscosity TPU/PLA blend and PLA were encapsulated by the low-viscosity TPU. In the samples composed of TPU

and TPU/PLA blend (Figure 7a–d), no significant change in morphology was observed according to the difference in the content of PLA in the TPU/PLA blend. However, at this time, fibers with a high PLA content in the TPU/PLA blend could better distinguish the interface with TPU. It is judged that this is because the same component between the two components is reduced in samples with a high content of PLA and a low content of TPU on the TPU/PLA blend. From this point of view, it was confirmed that these properties were more pronounced in sample (e), some of which consisted of pure PLA. This is considered due to the lack of interconnectivity between the two components, TPU and PLA, as there are no identical components. Nevertheless, it has been confirmed by previous studies [21,22] that carbamates and PLA in the HS of TPU can form hydrogen bonds and that TPU and PLA can have some compatibility because both have ester bonds. Therefore, in sample (e), it is judged that a composite fiber can be formed without being completely separated.

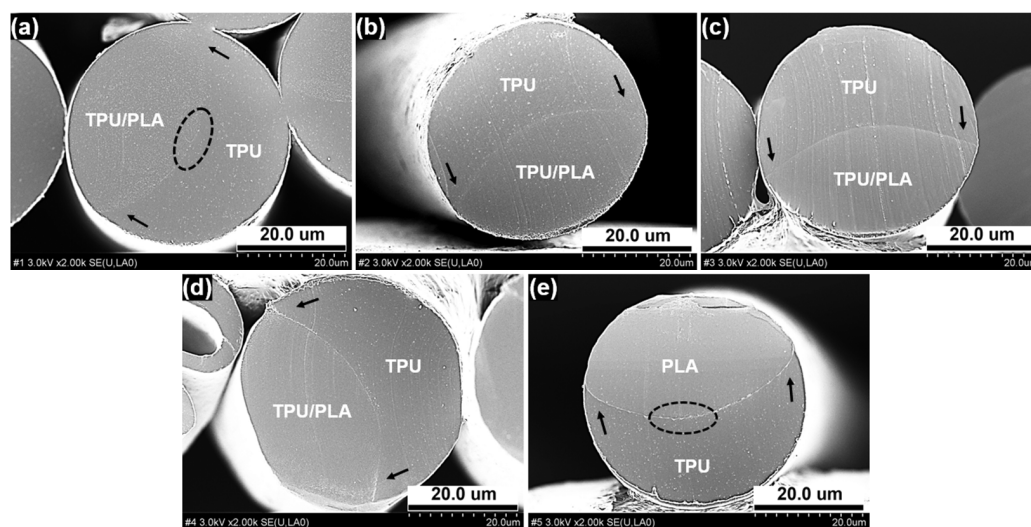


Figure 7. SEM image of TPU/(TPU/PLA), TPU/PLA side-by-side bicomponent fibers cross-section: (a) 50/(40/10), (b) 50/(30/20), (c) 50/(20/30), (d) 50/(10/40), and (e) 50/50. The arrows visualized the characteristic cross-sectional morphology of the bicomponent fiber.

Table 2 shows the biocarbon content of the (a)–(d) TPU/(TPU/PLA) and (e) TPU/PLA side-by-side bicomponent fibers. The biocarbon content of (e) TPU/PLA side-by-side bicomponent fiber was the highest at about 71.5% because PLA, a biodegradable biopolymer, contained the highest content. For TPU/(TPU/PLA) side-by-side bicomponent fibers, the sample with a PLA content of 10/40 was the highest among the TPU/PLA blends. Through this, we confirmed that the bio content of the final fiber could be improved by applying TPU/PLA blending with TPU.

Table 2. Biobased carbon contents of TPU/(TPU/PLA) and TPU/PLA side-by-side bicomponent fibers.

Samples	Biobased C (%)
(a) TPU/(TPU/PLA)_50/(40/10)	56.6
(b) TPU/(TPU/PLA)_50/(30/20)	59.2
(c) TPU/(TPU/PLA)_50/(20/30)	63.8
(d) TPU/(TPU/PLA)_50/(10/40)	68.4
(e) TPU/PLA_50/50	71.5

Figure 8 shows the FT–IR structural analysis spectrum for component and miscibility analysis of TPU/(TPU/PLA) bicomponent fibers. The vibrations of 3327 cm^{-1} and 1530 cm^{-1} appear due to the stretching and bending of the —NH bond in the urethane bond and the 1730 and 1703 cm^{-1} peaks corresponding to the C=O stretching of the urethane group are characteristic peaks of TPU [34]. These peaks were observed in (a)–(e) bicom-

ponent fibers, and the strength decreased with the addition of PLA. This consequently involves some molecular interactions within the blends [57,58]. The diversity of the weak bands around 3000 cm^{-1} seen in all (a)–(e) bicomponent fibers is due to the $-\text{CH}$ oscillation of the TPU [59,60]. In addition, a peak of 1596 cm^{-1} appears due to the presence of a benzene group in TPU [47]. On the other hand, in (e) bicomponent fiber composed of each TPU and PLA, strong peaks due to $-\text{CO}$ bonding of PLA were observed together at 1745 and 1081 cm^{-1} [58]. In addition, 2996 and 2920 cm^{-1} (asymmetric and symmetric, respectively) peaks due to the stretching vibrations of PLA appeared. Through these results, it was confirmed that the fibers were TPU/(TPU/PLA) and TPU/PLA bicomponent fibers.

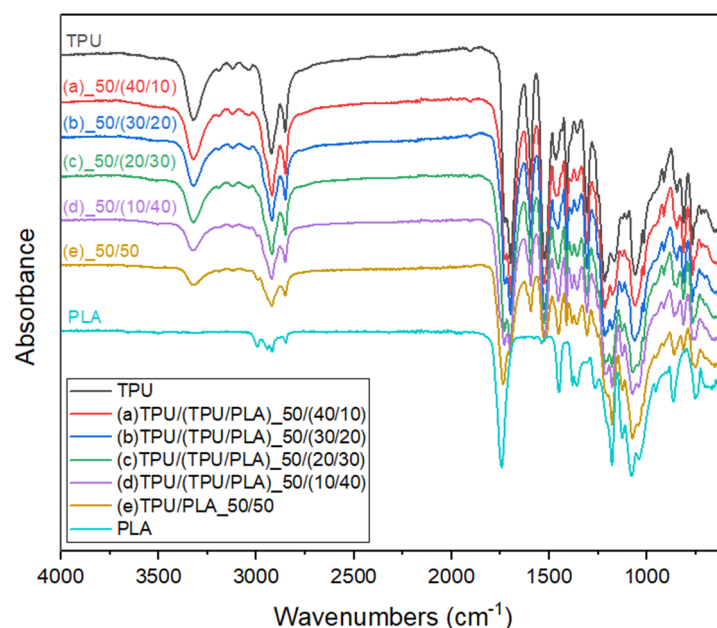


Figure 8. FT–IR spectra of TPU/(TPU/PLA) side-by-side bicomponent fibers ((a)–(e)), pure TPU, and PLA fibers.

DSC thermograms for the TPU and TPU/(TPU/PLA) side-by-side bicomponent fiber samples are shown in Figure 9, and the quantitative values are shown in Table 3. The endothermic peak observed at about $61\text{ }^{\circ}\text{C}$ of the bicomponent fiber samples ((a)–(e)) corresponds to the T_g on PLA, and the endothermic peak at about $149\text{ }^{\circ}\text{C}$ corresponds to the T_m . In addition, the exothermic peaks appearing at about $70\text{ }^{\circ}\text{C}$ in samples ((a)–(d)) except for (e) sample are related to the crystallization of the SS, and the double endothermic peaks at about $193\text{ }^{\circ}\text{C}$ and $218\text{ }^{\circ}\text{C}$ are attributed to the melting of the TPU phase [44,61]. Saiani et al. [62] proved these two endotherms were caused by the melting of the ordered structure appearing in the hard phase and microphase mixing of the soft and hard parts, respectively [63]. It is noteworthy that some different characteristics exist when comparing the (e) sample composed of pure TPU and PLA with samples ((a)–(d)) composed of TPU and TPU/PLA blends. The (e) sample showed a strong T_g peak of PLA, whereas samples ((a)–(d)) showed decreased T_g and crystallization temperature. Among the TPU/PLA blends, the sample containing more PLA content showed a stronger crystallization peak and X_c than TPU, and the (d) sample had the highest X_c value of 2.28%. For the TPU/PLA blend, it is speculated that the PLA present in the TPU amorphous matrix influenced the crystallization. In addition, the shoulder peak existing in the T_m section of PLA disappears and shows a sharp and narrow shape in samples ((a)–(d)), so it can be inferred that there is an interaction and compatibility between TPU and TPU/PLA. These results are consistent with the previous SEM results, and together with the FT-IR results, it was possible to confirm that the fibers were TPU/(TPU/PLA) bicomponent fibers.

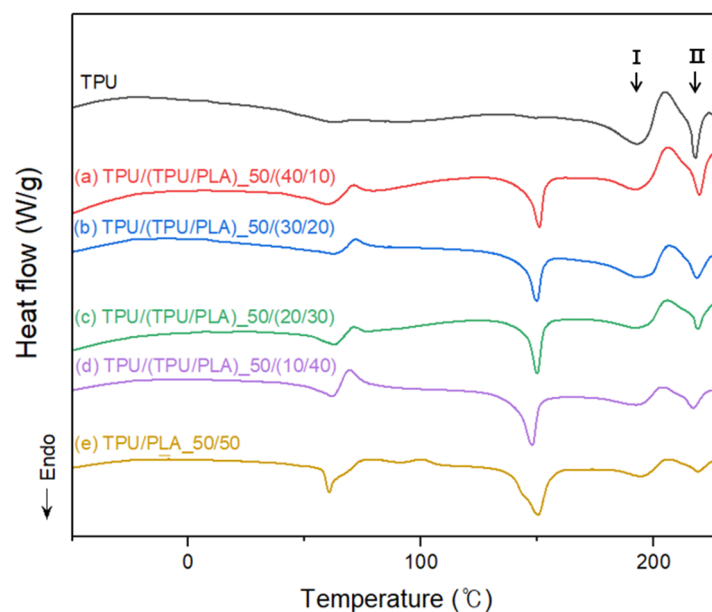


Figure 9. DSC thermograms of TPU fiber and TPU/(TPU/PLA) side-by-side bicomponent fibers ((a)–(e)). Two endothermic peaks (I, II) indicate the melting points of TPU.

Table 3. DSC characterization studies of TPU fiber and TPU/(TPU/PLA) side-by-side bicomponent fibers ((a)–(e)).

Samples	$T_{g, PLA}$ (°C)	T_c (°C)	$T_{m, PLA}$ (°C)	$T_{m, I}$ (°C)	$T_{m, II}$ (°C)	X_c (%)
TPU	-	69.62	-	193.29	217.92	0.44
(a) TPU/(TPU/PLA)_50/(40/10)	62.81	70.56	149.92	193.92	218.62	1.19
(b) TPU/(TPU/PLA)_50/(30/20)	62.97	70.95	149.75	193.22	218.42	1.70
(c) TPU/(TPU/PLA)_50/(20/30)	61.52	70.13	149.99	194.45	218.95	2.01
(d) TPU/(TPU/PLA)_50/(10/40)	61.45	70.01	149.85	193.46	217.89	2.28
(e) TPU/PLA_50/50	60.98	-	150.28	193.50	218.08	-

Figure 10 shows the stress–strain curves of TPU and TPU/(TPU/PLA) side-by-side fibers. The quantitative values of physical properties are summarized in Table 4. The stress–strain curves of side-by-side bicomponent fibers ((a)–(e)) were changed from the elastic behavior of TPU to partial plastic deformation characterized by the yield point [23]. The samples ((a)–(d)) showed increased tensile and yield strengths as the fibers composed of TPU/PLA blend with higher content of PLA with TPU. The modulus also tended to increase as the PLA content increased to 40%. Among them, sample (d) with a TPU/(TPU/PLA) ratio of 50/(10/40) had the highest tensile and yield strengths of 3624 and 1235 MPa, respectively. The modulus also increased the most to 3125 MPa. In other words, it can be seen that the PLA applied to the TPU/PLA blend can act as a reinforcing material to reinforce the TPU elastomer to improve the strength of the final fiber. On the other hand, in the case of the elongation at break, the opposite tendency was shown. This phenomenon is considered because PLA, which is present in the TPU/PLA blend among the side-by-side components, is a material with inherent brittleness and excellent strength. It is also noteworthy here, as in the FT-IR and DSC results, that in the case of the sample (e) in which pure TPU and PLA are in a 50/50 ratio, it can be seen that they exhibit unique behavior as they maintain the original properties of TPU and PLA, respectively. The initial curve showed a sharp increase in modulus and tensile strength like other bicomponent fibers, but after the yield point, the value was maintained with little change, and then the strain increased again by around 30%. This sample's tensile strength and yield strengths were 2152 and 909 MPa, respectively. Despite containing 50% pure PLA, it showed lower values of tensile strength than TPU fiber and lower yield strength than other samples ((b)–(d)).

In addition, the modulus is also 2979 MPa, indicating a lower value than the samples (c)–(d). These features may be related to the degradation of interfacial adhesion due to the lack of interconnectivity, as the presence of prominent boundaries between side-by-side fibrous TPU and PLA was confirmed in the SEM images. This is sufficiently predictable from previous studies [32] that the compositional difference between the two components should not be too large. Otherwise, they could separate, and the insufficient adhesion between the two components would not be able to withstand excessive mechanical forces.

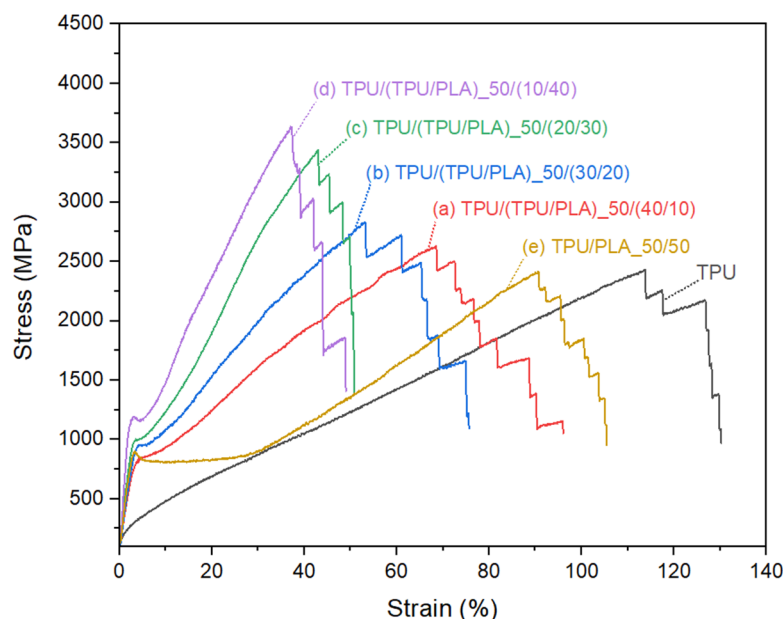


Figure 10. Stress–strain curves of TPU fiber and TPU(TPU/PLA) bicomponent fibers.

Table 4. Mechanical properties of TPU fiber and TPU(TPU/PLA) bicomponent fibers.

Samples	Tensile Strength (MPa)	Yield Strength (MPa)	Elongation at Break (%)	Young's Modulus (MPa)
TPU	2432 ± 114	-	113 ± 36	1452 ± 81
(a) TPU/(TPU/PLA)_50/(40/10)	2627 ± 101	864 ± 84	68 ± 11	2820 ± 60
(b) TPU/(TPU/PLA)_50/(30/20)	2796 ± 145	960 ± 26	53 ± 8	2880 ± 53
(c) TPU/(TPU/PLA)_50/(20/30)	3410 ± 113	994 ± 30	43 ± 5	3011 ± 45
(d) TPU/(TPU/PLA)_50/(10/40)	3624 ± 128	1235 ± 101	37 ± 4	3125 ± 49
(e) TPU/PLA_50/50	2152 ± 109	909 ± 54	90 ± 20	2979 ± 55

4. Conclusions

In this study, side-by-side bicomponent fibers composed of TPU, a bio-based raw material, and TPU/PLA blends were designed and characterized through melt spinning. To this end, two raw materials (TPU, TPU/PLA blends) were prepared for producing bicomponent fibers. TPU with M_w of 190,000 or more was synthesized based on biopolyester polyol, and blends were prepared in which TPU and PLA were mixed in different ratios. As a result, the presence of PLA in the prepared TPU/(TPU/PLA) side-by-side bicomponent fibers affected the physical properties along with the increase in the bio-content. PLA applied to the TPU/PLA blend acts as a reinforcing material to reinforce the TPU elastomer, improving the strength of the final fiber. Bicomponent fibers composed of a blend of TPU and TPU/PLA ratio of 10/40 showed increased tensile strength values up to 3624 MPa. On the other hand, side-by-side bicomponent fibers composed of pure PLA and TPU rather than a TPU/PLA blend had slightly different characteristics. At their side-by-side interface, the boundary was relatively clear, and the unique characteristics of TPU and PLA were observed in the FT-IR and DSC results. Among the prepared bicomponent

fibers, despite containing up to 50% of PLA, the tensile strength was lower than that of TPU fibers due to the deterioration of interconnectivity. Therefore, the presence of the same component between TPU and TPU/PLA blends affected the interfacial adhesion, resulting in improved physical properties. All these results indicate the successful preparation of TPU/(TPU/PLA) side-by-side bicomponent fibers with improved bio-content and tensile strength, and furthermore, they are expected to be applied to eco-friendly fiber applications. Moreover, it is expected that it will be able to play a sufficient role as a substitute for petroleum-based TPU used in the existing industry and apparel sector.

Author Contributions: Conceptualization, S.K.L.; formal analysis, H.-C.K.; funding acquisition, S.K.L. and S.-H.H.; investigation, J.O. and Y.K.K.; resources, J.-H.J. and C.-H.J.; writing—original draft, J.O.; writing—review, S.K.L., Y.K.K. and J.K. All authors have read and agreed to the published version of the manuscript.

Funding: This research was supported in 2022 by the Industrial Technology Innovation Program (Project no. 20010470) funded by the Ministry of Trade, Industry, and Energy (MOTIE, Korea) and the Korea Evaluation Institute of Industrial Technology (KEIT, Korea). Additionally, supported by the DGIST R&D program of the Ministry of Science and ICT of the Republic of Korea (grant number 22-ET-08).

Data Availability Statement: The data presented in this study are available on request from the corresponding author.

Conflicts of Interest: The authors declare no conflict of interest.

References

1. Varsavas, S.D.; Kaynak, C. Effects of glass fiber reinforcement and thermoplastic elastomer blending on the mechanical performance of polylactide. *Compos. Commun.* **2018**, *8*, 24–30. [[CrossRef](#)]
2. Nurul Fazita, M.R.; Jayaraman, K.; Bhattacharyya, D.; Mohamad Haafiz, M.K.; Saurabh, C.K.; Hussin, M.H.; H.P.S., A.K. Green composites made of bamboo fabric and poly (lactic) acid for packaging applications—A review. *Materials* **2016**, *9*, 435. [[CrossRef](#)] [[PubMed](#)]
3. Dicker, M.P.M.; Duckworth, P.F.; Baker, A.B.; Francois, G.; Hazzard, M.K.; Weaver, P.M. Green composites: A review of material attributes and complementary applications. *Compos. Part A* **2014**, *56*, 280–289. [[CrossRef](#)]
4. La Mantia, F.P.; Morreale, M. Green composites: A brief review. *Compos. Part A* **2011**, *42*, 579–588. [[CrossRef](#)]
5. Abdul Khalil, H.P.S.; Bhat, A.H.; Ireana Yusra, A.F. Green composites from sustainable cellulose nanofibrils: A review. *Carbohydr. Polym.* **2012**, *87*, 963–979. [[CrossRef](#)]
6. Eceiza, A.; Larrañaga, M.; de la Caba, K.; Kortaberria, G.; Marieta, C.; Corcuera, M.A.; Mondragon, I. Structure–property relationships of thermoplastic polyurethane elastomers based on polycarbonate diols. *J. Appl. Polym. Sci.* **2008**, *108*, 3092–3103. [[CrossRef](#)]
7. Gupta, T.K.; Singh, B.P.; Tripathi, R.K.; Dhakate, S.R.; Singh, V.N.; Panwar, O.S.; Mathur, R.B. Superior nano-mechanical properties of reduced graphene oxide reinforced polyurethane composites. *RSC Adv.* **2015**, *5*, 16921–16930. [[CrossRef](#)]
8. Delebecq, E.; Pascault, J.-P.; Boutevin, B.; Ganachaud, F. On the versatility of urethane/urea bonds: Reversibility, blocked isocyanate, and non-isocyanate polyurethane. *Chem. Rev.* **2013**, *113*, 80–118. [[CrossRef](#)]
9. Buckley, C.P.; Prisacariu, C.; Martin, C. Elasticity and inelasticity of thermoplastic polyurethane elastomers: Sensitivity to chemical and physical structure. *Polymer* **2010**, *51*, 3213–3224. [[CrossRef](#)]
10. Qi, H.J.; Boyce, M.C. Stress–strain behavior of thermoplastic polyurethanes. *Mech. Mater.* **2005**, *37*, 817–839. [[CrossRef](#)]
11. Xu, C.; Huang, Y.; Tang, L.; Hong, Y. Low-initial-modulus biodegradable polyurethane elastomers for soft tissue regeneration. *ACS Appl. Mater. Interfaces* **2017**, *9*, 2169–2180. [[CrossRef](#)] [[PubMed](#)]
12. Kucinska-Lipka, J.; Gubanska, I.; Janik, H.; Sienkiewicz, M. Fabrication of polyurethane and polyurethane based composite fibres by the electrospinning technique for soft tissue engineering of cardiovascular system. *Mater. Sci. Eng. C* **2015**, *46*, 166–176. [[CrossRef](#)] [[PubMed](#)]
13. Im, H.G.; Ka, K.R.; Kim, C.K. Characteristics of polyurethane elastomer blends with poly(acrylonitrile-co-butadiene) rubber as an encapsulant for underwater sonar devices. *Ind. Eng. Chem. Res.* **2010**, *49*, 7336–7342. [[CrossRef](#)]
14. Feng, F.; Ye, L. Morphologies and mechanical properties of polylactide/thermoplastic polyurethane elastomer blends. *J. Appl. Polym. Sci.* **2011**, *119*, 2778–2783. [[CrossRef](#)]
15. Tan, L.; Su, Q.; Zhang, S.; Huang, H. Preparing thermoplastic polyurethane/thermoplastic starch with high mechanical and biodegradable properties. *RSC Adv.* **2015**, *5*, 80884–80892. [[CrossRef](#)]
16. Akindoyo, J.O.; Beg, M.D.H.; Ghazali, S.; Islam, M.R.; Jeyaratnam, N.; Yuvaraj, A.R. Polyurethane types, synthesis and applications—A review. *RSC Adv.* **2016**, *6*, 114453–114482. [[CrossRef](#)]

17. Zhang, C.; Kessler, M.R. Bio-based polyurethane foam made from compatible blends of vegetable-oil-based polyol and petroleum-based polyol. *ACS Sustain. Chem. Eng.* **2015**, *3*, 743–749. [[CrossRef](#)]
18. Sawpan, M.A. Polyurethanes from vegetable oils and applications: A review. *J. Polym. Res.* **2018**, *25*, 184. [[CrossRef](#)]
19. Zhang, C.; Wang, H.; Zeng, W.; Zhou, Q. High biobased carbon content polyurethane dispersions synthesized from fatty acid-based isocyanate. *Ind. Eng. Chem. Res.* **2019**, *58*, 5195–5201. [[CrossRef](#)]
20. Pillai, P.K.S.; Floros, M.C.; Narine, S.S. Elastomers from renewable metathesized palm oil polyols. *ACS Sustainable Chem. Eng.* **2017**, *5*, 5793–5799. [[CrossRef](#)]
21. Li, Y.; Shimizu, H. Toughening of polylactide by melt blending with a biodegradable poly(ether)urethane elastomer. *Macromol. Biosci.* **2007**, *7*, 921–928. [[CrossRef](#)] [[PubMed](#)]
22. Jašo, V.; Cvetinov, M.; Rakić, S.; Petrović, Z.S. Bio-plastics and elastomers from polylactic acid/thermoplastic polyurethane blends. *J. Appl. Polym. Sci.* **2014**, *131*, 41104. [[CrossRef](#)]
23. Jašo, V.; Rodić, M.V.; Petrović, Z.S. Biocompatible fibers from thermoplastic polyurethane reinforced with polylactic acid microfibers. *Eur. Polym. J.* **2015**, *63*, 20–28. [[CrossRef](#)]
24. Hong, H.; Wei, J.; Yuan, Y.; Chen, F.-P.; Wang, J.; Qu, X.; Liu, C.-S. A novel composite coupled hardness with flexibility—Polylactic acid toughen with thermoplastic polyurethane. *J. Appl. Polym. Sci.* **2011**, *121*, 855–861. [[CrossRef](#)]
25. Naeimirad, M.; Zadhoush, A.; Kotek, R.; Esmaeely Neisiany, R.; Nouri Khorasani, S.; Ramakrishna, S. Recent advances in core/shell bicomponent fibers and nanofibers: A review. *J. Appl. Polym. Sci.* **2018**, *135*, 46265. [[CrossRef](#)]
26. Hufenus, R.; Affolter, C.; Camenzind, M.; Reifler, F.A. Design and characterization of a bicomponent melt-spun fiber optimized for artificial turf applications. *Macromol. Mater. Eng.* **2013**, *298*, 653–663. [[CrossRef](#)]
27. Tallury, S.S.; Pourdeyhimi, B.; Pasquinelli, M.A.; Spontak, R.J. Physical microfabrication of shape-memory polymer systems via bicomponent fiber spinning. *Macromol. Rapid Commun.* **2016**, *37*, 1837–1843. [[CrossRef](#)]
28. Yan, X.; Yu, M.; Ramakrishna, S.; Russell, S.J.; Long, Y.-Z. Advances in portable electrospinning devices for in situ delivery of personalized wound care. *Nanoscale* **2019**, *11*, 19166–19178. [[CrossRef](#)]
29. Gupta, P.; Wilkes, G.L. Some investigations on the fiber formation by utilizing a side-by-side bicomponent electrospinning approach. *Polymer* **2003**, *44*, 6353–6359. [[CrossRef](#)]
30. Peng, H.; Xie, R.; Fang, K.; Cao, C.; Qi, Y.; Ren, Y.; Chen, W. Effect of diethylene glycol on the inkjet printability of reactive dye solution for cotton fabrics. *Langmuir* **2021**, *37*, 1493–1500. [[CrossRef](#)]
31. Wang, H.; Wang, X.; Fan, T.; Zhou, R.; Li, J.; Long, Y.; Zhuang, X.; Cheng, B. Fabrication of electrospun sulfonated poly(ether sulfone) nanofibers with amino modified SiO₂ nanosphere for optimization of nanochannels in proton exchange membrane. *Solid State Ionics* **2020**, *349*, 115300. [[CrossRef](#)]
32. Zhu, S.; Meng, X.; Yan, X.; Chen, S. Evidence for bicomponent fibers: A review. *e-Polymers* **2021**, *21*, 636–653. [[CrossRef](#)]
33. Pattamaprom, C.; Wu, C.-H.; Chen, P.-H.; Huang, Y.-L.; Ranganathan, P.; Rwei, S.-P.; Chuan, F.-S. Solvent-free one-shot synthesis of thermoplastic polyurethane based on bio-poly(1,3-propylene succinate) glycol with temperature-sensitive shape memory behavior. *ACS Omega* **2020**, *5*, 4058–4066. [[CrossRef](#)] [[PubMed](#)]
34. Charlon, M.; Heinrich, B.; Matter, Y.; Couzigné, E.; Donnio, B.; Averous, L. Synthesis, structure and properties of fully biobased thermoplastic polyurethanes, obtained from a diisocyanate based on modified dimer fatty acids, and different renewable diols. *Eur. Polym. J.* **2014**, *61*, 197–205. [[CrossRef](#)]
35. Oh, J.; Kim, Y.K.; Hwang, S.-H.; Kim, H.-C.; Jung, J.-H.; Jeon, C.-H.; Kim, J.; Lim, S.K. Synthesis of thermoplastic polyurethanes containing bio-based polyester polyol and their fiber property. *Polymers* **2022**, *14*, 2033. [[CrossRef](#)] [[PubMed](#)]
36. Parcheta, P.; Głowińska, E.; Datta, J. Effect of bio-based components on the chemical structure, thermal stability and mechanical properties of green thermoplastic polyurethane elastomers. *Eur. Polym. J.* **2020**, *123*, 109422. [[CrossRef](#)]
37. Haverly, M.R.; Fenwick, S.R.; Patterson, F.P.K.; Slade, D.A. Biobased carbon content quantification through AMS radiocarbon analysis of liquid fuels. *Fuel* **2019**, *237*, 1108–1111. [[CrossRef](#)]
38. Sánchez-Calderón, I.; Bernardo, V.; Santiago-Calvo, M.; Naji, H.; Saiani, A.; Rodríguez-Pérez, M.Á. Effect of the molecular structure of tpu on the cellular structure of nanocellular polymers based on pmma/tpu blends. *Polymers* **2021**, *13*, 3055. [[CrossRef](#)]
39. Bockorny, G.d.A.; Forte, M.M.C.; Stamboroski, S.; Noeske, M.; Keil, A.; Leite Cavalcanti, W. Modifying a thermoplastic polyurethane for improving the bonding performance in an adhesive technical process. *Appl. Adhes. Sci.* **2016**, *4*, 4. [[CrossRef](#)]
40. Ng, H.N.; Allegranza, A.E.; Seymour, R.W.; Cooper, S.L. Effect of segment size and polydispersity on the properties of polyurethane block polymers. *Polymer* **1973**, *14*, 255–261. [[CrossRef](#)]
41. Hu, W.; Koberstein, J.T. The effect of thermal annealing on the thermal properties and molecular weight of a segmented polyurethane copolymer. *J. Polym. Sci. Part B: Polym. Phys.* **1994**, *32*, 437–446. [[CrossRef](#)]
42. Kwei, T.K. Phase separation in segmented polyurethanes. *J. Appl. Polym. Sci.* **1982**, *27*, 2891–2899. [[CrossRef](#)]
43. Lin, S.B.; Hwang, K.S.; Tsay, S.Y.; Cooper, S.L. Segmental orientation studies of polyether polyurethane block copolymers with different hard segment lengths and distributions. *Colloid Polym. Sci.* **1985**, *263*, 128–140. [[CrossRef](#)]
44. Hundiwale, D.G.; Kapadi, U.R.; Pandya, M.V. Effect of macroglycol structure and its molecular weight on physicomechanical properties of polyurethanes. *J. Appl. Polym. Sci.* **1995**, *55*, 1329–1333. [[CrossRef](#)]
45. Sohn, M.H.; Li, X.X.; Cho, U.R. Synthesis of polyurethane elastomers by different kinds of acids. *Polymer* **2019**, *43*, 824–830.
46. Kaushik, A.; Ahuja, D.; Salwani, V. Synthesis and characterization of organically modified clay/castor oil based chain extended polyurethane nanocomposites. *Compos. Part A* **2011**, *42*, 1534–1541. [[CrossRef](#)]

47. Liu, Z.; Wu, B.; Jiang, Y.; Lei, J.; Zhou, C.; Zhang, J.; Wang, J. Solvent-free and self-catalysis synthesis and properties of waterborne polyurethane. *Polymer* **2018**, *143*, 129–136. [[CrossRef](#)]
48. Irusta, L.; Fernandez-Berridi, M.J. Aromatic poly(ester–urethanes): Effect of the polyol molecular weight on the photochemical behaviour. *Polymer* **2000**, *41*, 3297–3302. [[CrossRef](#)]
49. Kaushiva, B.D.; McCartney, S.R.; Rossmly, G.R.; Wilkes, G.L. Surfactant level influences on structure and properties of flexible slabstock polyurethane foams. *Polymer* **2000**, *41*, 285–310. [[CrossRef](#)]
50. Senich, G.A.; MacKnight, W.J. Fourier transform infrared thermal analysis of a segmented polyurethane. *Macromolecules* **1980**, *13*, 106–110. [[CrossRef](#)]
51. Ahmed, M.F.; Li, Y.; Yao, Z.; Cao, K.; Zeng, C. TPU/PLA blend foams: Enhanced foamability, structural stability, and implications for shape memory foams. *J. Appl. Polym. Sci.* **2019**, *136*, 47416. [[CrossRef](#)]
52. Sharudin, R.W.B.; Ohshima, M. Preparation of microcellular thermoplastic elastomer foams from polystyrene-*b*-ethylene-butylene-*b*-polystyrene (SEBS) and their blends with polystyrene. *J. Appl. Polym. Sci.* **2013**, *128*, 2245–2254. [[CrossRef](#)]
53. Song, J.J.; Chang, H.H.; Naguib, H.E. Design and characterization of biocompatible shape memory polymer (SMP) blend foams with a dynamic porous structure. *Polymer* **2015**, *56*, 82–92. [[CrossRef](#)]
54. Kanbur, Y.; Tayfun, U. Development of multifunctional polyurethane elastomer composites containing fullerene: Mechanical, damping, thermal, and flammability behaviors. *J. Elastomers Plast.* **2018**, *51*, 262–279. [[CrossRef](#)]
55. Karagiannis, A.; Mavridis, H.; Hrymak, A.N.; Vlachopoulos, J. Interface determination in bicomponent extrusion. *Polym. Eng. Sci.* **1988**, *28*, 982–988. [[CrossRef](#)]
56. Ayad, E.; Cayla, A.; Rault, F.; Gonthier, A.; LeBlanc, T.; Campagne, C.; Devaux, E. Influence of rheological and thermal properties of polymers during melt spinning on bicomponent fiber morphology. *J. Mater. Eng. Perform.* **2016**, *25*, 3296–3302. [[CrossRef](#)]
57. Oliaei, E.; Kaffashi, B.; Davoodi, S. Investigation of structure and mechanical properties of toughened poly(l-lactide)/thermoplastic poly(ester urethane) blends. *J. Appl. Polym. Sci.* **2016**, *133*, 43104. [[CrossRef](#)]
58. Siahsharani, A.; Behraves, A.H.; Barmouz, M. Compressive shape memory behavior of spring-shaped polylactic acid alloy type. *J. Appl. Polym. Sci.* **2017**, *134*, 45115. [[CrossRef](#)]
59. Kaynak, C.; Meyva, Y. Use of maleic anhydride compatibilization to improve toughness and other properties of polylactide blended with thermoplastic elastomers. *Polym. Adv. Technol.* **2014**, *25*, 1622–1632. [[CrossRef](#)]
60. Davachi, S.M.; Kaffashi, B. Preparation and characterization of poly l-lactide/triclosan nanoparticles for specific antibacterial and medical applications. *Int. J. Polym. Mater. Polym. Biomater.* **2015**, *64*, 497–508. [[CrossRef](#)]
61. Shakouri, Z.; Nazockdast, H. Microstructural development and mechanical performance of pla/tpu blends containing geometrically different cellulose nanocrystals. *Cellulose* **2018**, *25*, 7167–7188. [[CrossRef](#)]
62. Saiani, A.; Daunch, W.A.; Verbeke, H.; Leenslag, J.W.; Higgins, J.S. Origin of multiple melting endotherms in a high hard block content polyurethane. 1. Thermodynamic investigation. *Macromolecules* **2001**, *34*, 9059–9068. [[CrossRef](#)]
63. Yahiaoui, M.; Denape, J.; Paris, J.Y.; Ural, A.G.; Alcalá, N.; Martínez, F.J. Wear dynamics of a tpu/steel contact under reciprocal sliding. *Wear* **2014**, *315*, 103–114. [[CrossRef](#)]